Mechanical Properties of Linseed Oil Monoglyceride Maleate/Styrene Copolymers

M. Mosiewicki, M. I. Aranguren, J. Borrajo

Institute of Materials Science and Technology (INTEMA), University of Mar del Plata - National Research Council (CONICET), Av. Juan B. Justo 4302, (7600) Mar del Plata, Argentina

ABSTRACT: In this study, rigid thermoset polymers were prepared from radical copolymerization of linseed oil monoglyceride maleates with styrene (St). First, linseed oil monoglycerides (LOMGs) were obtained from the reaction of linseed oil with glycerol at 220–240°C. Then, LOMGs were reacted with maleic anhydride at 80°C to produce the LOMG maleate half esters. The reactions were followed by FTIR spectroscopy and size exclusion chromatography (SEC) and the final resin was characterized by ^{1}H-NMR spectroscopy. Finally, radical copolymerization of the LOMG maleates with 20, 40, 60, and 80% by weight of St was performed to produce rigid, thermoset polymers. The thermomechanical properties and fracture behavior of the cured copolymers, as a function of the percentage of St, were measured and analyzed. The copolymer with 40% by weight of St was the material with better mechanical and fracture behavior. © 2005 Wiley Periodicals, Inc. J Appl Polym Sci 97: 825–836, 2005

Key words: linseed oil; linseed oil monoglyceride; monoglyceride maleates; thermal properties; mechanical properties

INTRODUCTION

Polymers prepared from renewable natural resources have become increasingly important because of their low cost, availability, and potential biodegradability.[1]

Plant oils are triglycerides with numerous active sites amenable to chemical reactions to be converted to useful polymeric materials.[2] Their use in alkyl resin manufacture is well known. It involves the alcoholysis of the oil with a polyhydric alcohol to be used as the diol component in the polyesterification reaction with various diacids and anhydrides.[3] Furthermore, there have been many works that reported the direct cationic polymerization or copolymerization of the C=C bonds of the oil fatty acid side chains.[4–6] However, with various comonomers, such as styrene or divinylbenzene, the unsaturated bonds on fatty acid chains of triglycerides are not active in radical polymerization.

Since the double bonds in the fatty acid main chain are unable to homopolymerize,[6] and since they show low reactivity, an interesting alternative is to modify the triglyceride structure attaching reactive groups to it. Wool and coworkers[7] have prepared rigid thermosetting polymers by the free radical copolymerization of soybean oil monoglyceride maleates with styrene. In this work, linseed oil was used instead of soybean oil, and the corresponding monoglyceride maleates were obtained by glycerol transesterification of linseed oil, followed by esterification with maleic anhydride to half esters. The resulting polyfunctional monomer was free radically copolymerized with a reactive diluent such as styrene (Fig. 1). This synthetic route seems to be an interesting alternative to replace unsaturated polyester or vinyl ester resins synthesized from petroleum-based chemicals.

The objective of the present work was to prepare rigid thermosetting polymers from linseed oil. Linseed oil is commercially used as a drying oil in paints and protective coatings. Its high content of linoleic acid allows it to dry (a slow and gradual process of autooxidation) to form a tough, flexible film.[8]

In this study, the synthesized linseed oil monoglyceride maleate was reacted with styrene by free radical copolymerization. The mechanical properties and fracture behavior of the resulting network were analyzed as a function of the concentration of styrene in the reactive mixture.

EXPERIMENTAL

Materials

The linseed oil used was provided by Grainer S.A. (Entre Rios, Argentine) and was used without further purification. The glycerol used was 99.5% pure and was obtained from Científica Central (Bs. As., Argentine). A commercial soap without additives was used as emulsifier catalyst for this reaction. In the maleinization reaction, maleic anhydride and 2-methyl imidazole, as a catalyst, both from Fluka, were used. The
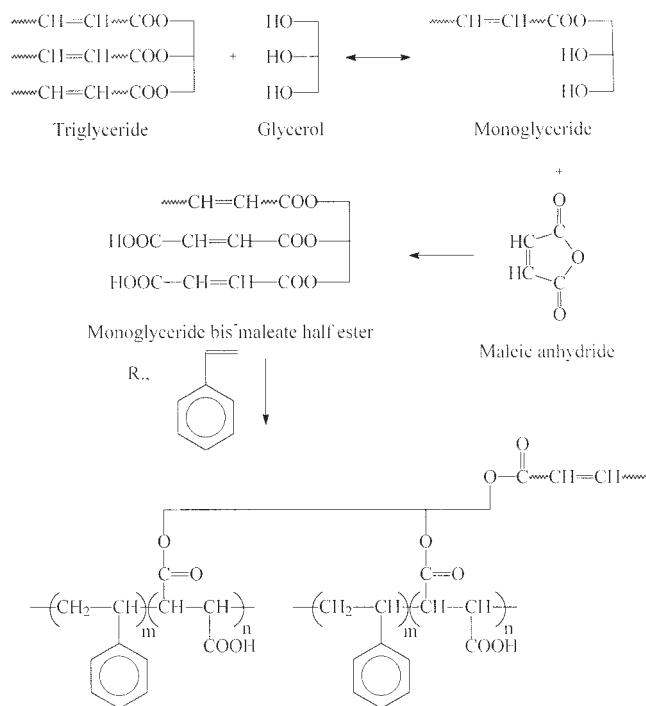

Figure 1 Synthesis and polymerization of linseed oil monoglyceride maleates.

radical initiator was benzoyl peroxide (Lucidol 0.75, Akzo Chemical S.A).

Synthesis of linseed oil monoglyceride (LOMG) maleates

Glycerolysis of linseed oil

Glycerol was heated at 220–230°C for 2 h under N_2 atmosphere before glycerolysis to remove trace amounts of water. The glycerolysis reaction was carried out using a weight ratio of 2 g of linseed oil to 1g of glycerol. Then, the linseed oil was added in five steps at 1 h intervals. A commercial soap (1% wt.) was also added, and the solution was heated for 5.5 h at 220–230°C. After that, the reaction flask was cooled by immersion in an ice and salt mixture down to room temperature. Approximately 50% of the initial excess of glycerol was removed.

Maleinization of LOMG

The conditions for reaction were adapted from the work of Wool and coworkers[6] on the optimization of the reaction variables for the maleinization of soybean oil monoglycerides.

The glyceride/glycerol mixture and the maleic anhydride were loaded at a 1.5 : 1 weight ratio in a reactor equipped with a mechanical stirrer and heated at 80°C for 5.5 h. Then, 0.6% wt. of 2-methyl imidazole (catalyst) and 500 ppm of hydroquinone (free radical inhibitor used to protect maleate unsaturations) were added to the mixture. FTIR data showed that the maleic anhydride was totally consumed after reaction. The final product was a viscous liquid and was stored in a refrigerator (8°C).

Preparation of the styrene copolymers

The linseed oil resin was mixed with 20, 40, 60, and 80% (by weight) of St and 2.5% (by weight) of benzoyl peroxide. The solution was heated to 40–50°C to achieve homogeneity. The mixture-filled mold was placed in an oven at 50°C for 2 h, and the temperature was increased at the rate of 1°C/min up to 90°C. Curing took place at this temperature for 1.5 h, and the sample was postcured at 150°C for another 1.5 h.

Two types of molds were used. To obtain plaques the reactive mixtures were poured between two plane glasses separated by a rubber cord and kept closed with metal clamps. To obtain cylinders, glass tubes of 5 mm of interior diameter were used. In both cases, the molds were previously treated with silicone release agent.

Methods and techniques

Physical characterization of the resin

A set of glass tubes, containing known masses of the reacting mixture in the range of 8–25 mg, were removed at predetermined times during the resin synthesis, their contents were dissolved in 5 mL tetrahydrofuran (THF), and 25 μL of the resulting solution injected in the size exclusion chromatograph (SEC, Waters 510 with HR 0.5, 1, and 3 ultrastyragel columns, UV detector at 240 nm, and a THF flow rate of 1 mL/min).

The samples were also characterized by transmission FTIR spectroscopy, using windows of NaCl. All spectra were recorded at 2 cm^{-1} resolutions with the use of a Genesis II Fourier transform infrared spectrometer. Results reported were the average of 16 scans.

^{1}H-NMR spectrum was recorded using a Bruker AM500 (500 MHz) equipped with a broadband probe using deuterated dimethylketone (CD_3COCD_3) as a solvent.

The efficiency of the maleinization was determined by using analytical techniques (acid number and saponification values).[9]

Mechanical testing of the cured materials

The final properties of the LOMG maleates/St copolymers were determined using dynamic-mechanical, tensile, compression, and flexural tests.

Dynamic-Mechanical Tests were performed using a Perkin–Elmer dynamic mechanical analyzer, DMA 7e, using the three point bending fixture (specimen plat-

form of 15 mm length) under nitrogen atmosphere. The specimens were cut to $20 \times 3 \times 2$ mm^3. The dynamic and static stresses were kept at 100 and 50 KPa, respectively. The frequency of the forced oscillations was fixed at 1 Hz, and the heating rate was 10°C/min. At least two replicate determinations were made for each sample to ensure the reproducibility of results.

The tensile tests were conducted using dog-bone specimens in accordance with ASTM D638*M* (sample type 4). The length of the narrow straight section in the specimens was 5 mm. The toughness of the polymer, corresponding to the fracture energy per unit volume of the sample, was obtained from the area under the corresponding tensile stress–strain curve.[10]

Uniaxial static compression tests were carried out to determine the modulus, yield stress, and ultimate stress in samples with different compositions. Compression specimens were obtained from samples molded in glass tubes of 5 mm of internal diameter coated with silicone release agent. Cylinders were cut with a height/diameter ratio of 1.5 to 2.0 (ASTM D695*M*). The top and bottom faces were carefully machined to be parallel, and the dimensions were measured with a caliper up to ± 0.01 mm.

Three-point bending tests were performed in accordance with ASTM D790–93 standard (sample type 1). Specimens of approximately $6 \times 10 \times 10$ mm^3 were cut from the molded plates for testing. The bending moduli were determined from the stress–strain curves.

All the static tests were carried out at a crosshead speed of 2 mm/min and room temperature using an Instron 8501 universal testing machine. At least four specimens of each sample were conditioned and tested.

Fracture behavior

Thick plates for fracture measurements were obtained by casting the mixture into a mold consisting of two glass plates with an adhered PET film acting as release agent, spaced by a 6 mm Teflon piece (thickness of the specimens) and held together with clamps. The specimens were prepared by cutting rectangular bars with a diamond saw. Central V-shaped notches were machined in the bars, then a fresh razor blade was slid in the notch to induce the growth of a natural crack ahead of the blade. The samples tested were those showing a total crack length, a, in the range of 0.45 < a/W < 0.55, where W is the width of the specimen (Fig. 2). The span to width (S/W) and the thickness to width (B/W) ratios were kept equal to 4 and 0.5, respectively.

Fracture tests were conducted at room temperature, in the three-point bending mode at a crosshead displacement rate of 2 mm/min, using the universal testing machine mentioned above. Values of K_{IQ} were
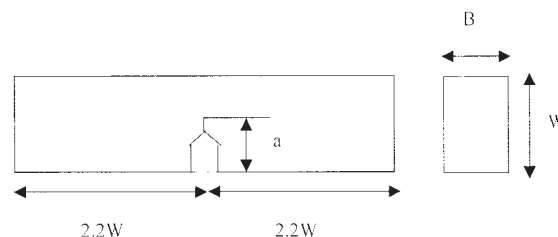

Figure 2 Fracture test configuration.

obtained using the standard norm D5045–93, for single-edge-notch bending (SENB) geometry, as:

$$K_{IQ} = \frac{f \cdot P_Q}{B \cdot W^{0.5}} \quad (1)$$

where

$$f = 6 \frac{a^{0.5}}{W} \left\{ 1.99 - \left(\frac{a}{W}\right) \cdot \left(1 - \frac{a}{W}\right) \cdot \left[2.15 \right. \right.$$
$$\left. \left. - 3.93 \cdot \left(\frac{a}{W}\right) + 2.7 \cdot \left(\frac{a}{W}\right)^2 \right] \right\} \left[1 + 2 \cdot \left(\frac{a}{W}\right) \right]$$
$$\cdot \left[1 - \left(\frac{a}{W}\right) \right]^{1.5} \quad (2)$$

and P_Q = load at crack initiation.

When the curve of load versus load point displacement is a straight line with an abrupt drop of load to zero at the instant of crack initiation, P_Q is the maximum load. However, when some nonlinearity is displayed, the true initiation load is not defined by the maximum and an arbitrary rule is generally used.[11] The best straight line should be drawn to determine the initial compliance, C. This value is then increased by 5% and a new line is drawn, $C_{5\%}$. If P_{max} falls within these two lines, then P_{max} is used to find K_{IQ}. If there is no maximum in the load curve up to the $C_{5\%}$-line intercept, then $P_{5\%}$ is found and this value is taken as the load at crack initiation, P_Q.

Besides, the work of fracture (wof) was also evaluated from:

$$\text{wof} = \frac{W_{\text{wof}}}{2 \cdot B \cdot (W - a)}$$

where W_{wof} is the total fracture energy determined from the total area under the load-displacement curve. The work of fracture gives the energy necessary for driving the crack through the whole sample and takes into account differences in crack propagation modes, including the strain energy release rate evaluated at its propagation value, according to methodology proposed by Adams and colleagues.[12]
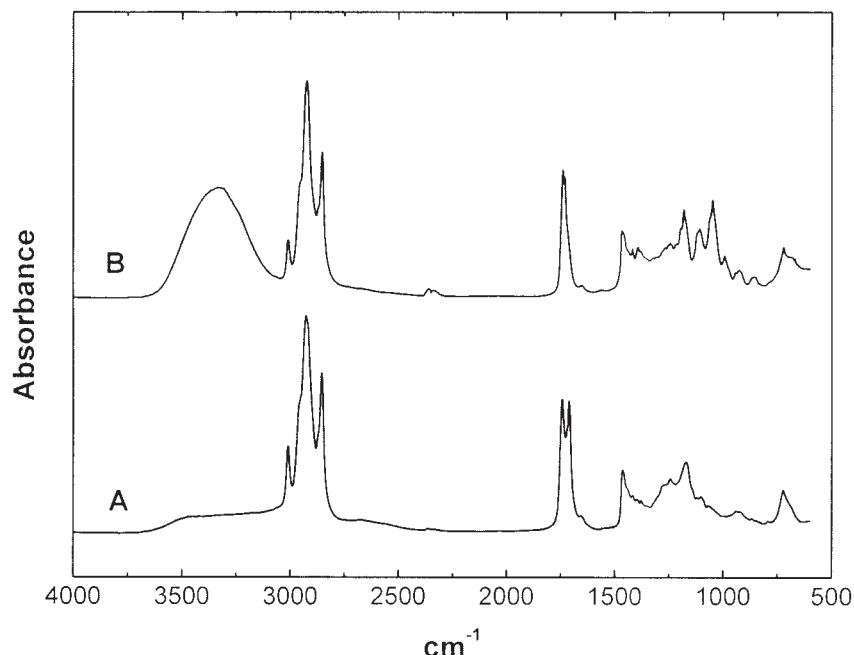
Figure 3 FTIR spectra of linseed oil (curve A) and LOMG (curve B).

The total crack length was measured from the fracture surface, using a profile projector with a magnification of 10×.

Fracture properties reported are the result of averaging at least eight specimens.

The surfaces of fractures were analyzed using optical microscopy Olympus SZH 10.

RESULTS AND DISCUSSION

Resin formulation and characterization

The glycerolysis of triglycerides is a reversible reaction, so to maximize the monoglyceride yield an excess of glycerol was used. This is limited by the solubility of glycerol in the triglyceride. To provide intimate contact between the triglyceride and glycerol phases, glycerol was emulsified in the triglyceride by using soap as an emulsifier.[7]

The equilibrium is favorable for monoglyceride formation at high temperatures. But, as the reaction temperature decreases, the excess glycerol tends to separate from the reaction mixture, which favors the transesterification back to triglycerides. So to prevent the reversion at the end of the reaction, the mixture was rapidly cooled to a temperature where all transesterification reactions have a negligible rate.

All the steps of the synthesis of the resins were followed by FTIR spectroscopy and GPC chromatography by taking samples at different reaction times. Also, the saponification index of the samples was determined, and the final resin was characterized analytically using ^{1}H-NMR spectroscopy.

Figure 3 shows the FTIR spectra of linseed oil (curve A) and LOMG (curve B), and Table I includes the peak assignments. The LOMGs spectra presents a large increase (with respect to the original oil) of the absorption band located at 3500 cm^{-1}, which is due to the OH presence in the glycerolysis product.

The band at 3011 cm^{-1}, which is assigned to the absorption of C=C bonds, appears in both spectra, indicating that unsaturation was preserved during the glycerolysis reaction.

The linseed oil spectrum shows a peak at 1710 cm^{-1}, which belongs to the stretch ν(C=O) of carboxylic acids, so the linseed oil contains free acids originated by the hydrolysis of the triglycerides during storage.

TABLE I
Band Assignment for the Infrared Absorbtion of Linseed Oil and LOMG

	Band position (cm^{-1})	
Assignment	Linseed oil	LOMG
ν(OH) m	—	3650–3590
ν(C=C—H) s	3011	3011
ν(CH, CH$_2$, CH$_3$) m	2924–2850	2923–2853
ν(C=O) s	1742	1739
ν(C=O) free acid s	1711	—
ν(C=C) vinyl m	1647	1635
δ(CH, CH$_2$, CH$_3$) m	1463	1466
νCH$_2$(C=O)	1418	1418
ν (C—O) s	1242	1242
δ(O—H)	—	1107–1047
ν (C—O—C) s	1165	1180
δ(C=C) vinyl m	923	923
—C—(CH$_2$)—C—	717	720

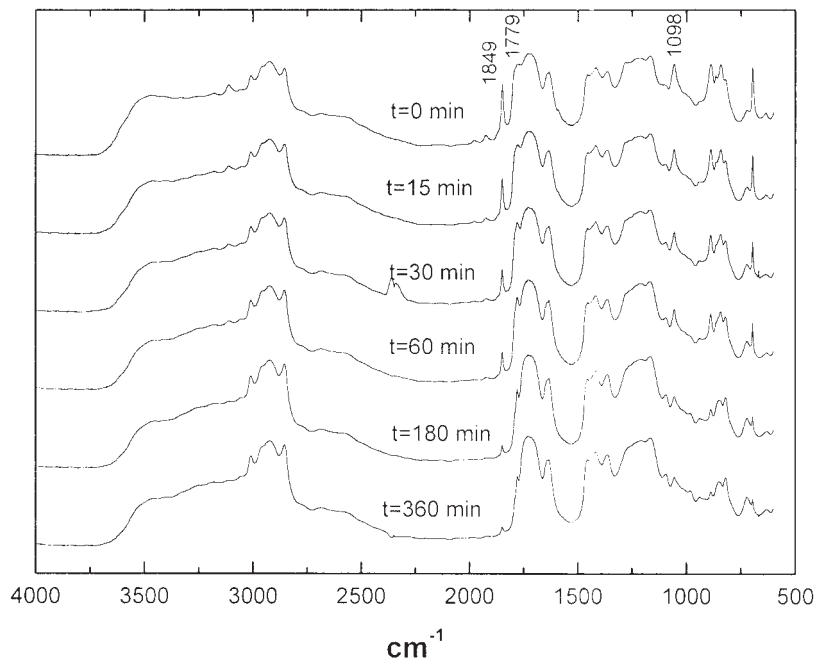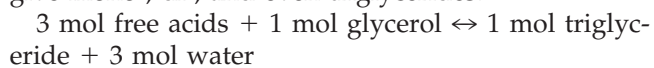ν, stretching; δ, deformation; s, strong; m, medium.

Figure 4 FTIR spectra of samples taken at different maleinization reaction times.

The LOMG spectrum (FTIR) does not show any free acid because of its reaction with glycerol in excess to give mono-, di-, and even triglycerides:

3 mol free acids + 1 mol glycerol ↔ 1 mol triglyceride + 3 mol water

The peaks at 1242 and 1742 cm^{-1}, corresponding to the absorption of the ester bonds in the triglycerides (curve A), decrease after glycerolysis (curve B).

Figure 4 shows FTIR spectra of samples taken at different maleinization reaction times. There is a
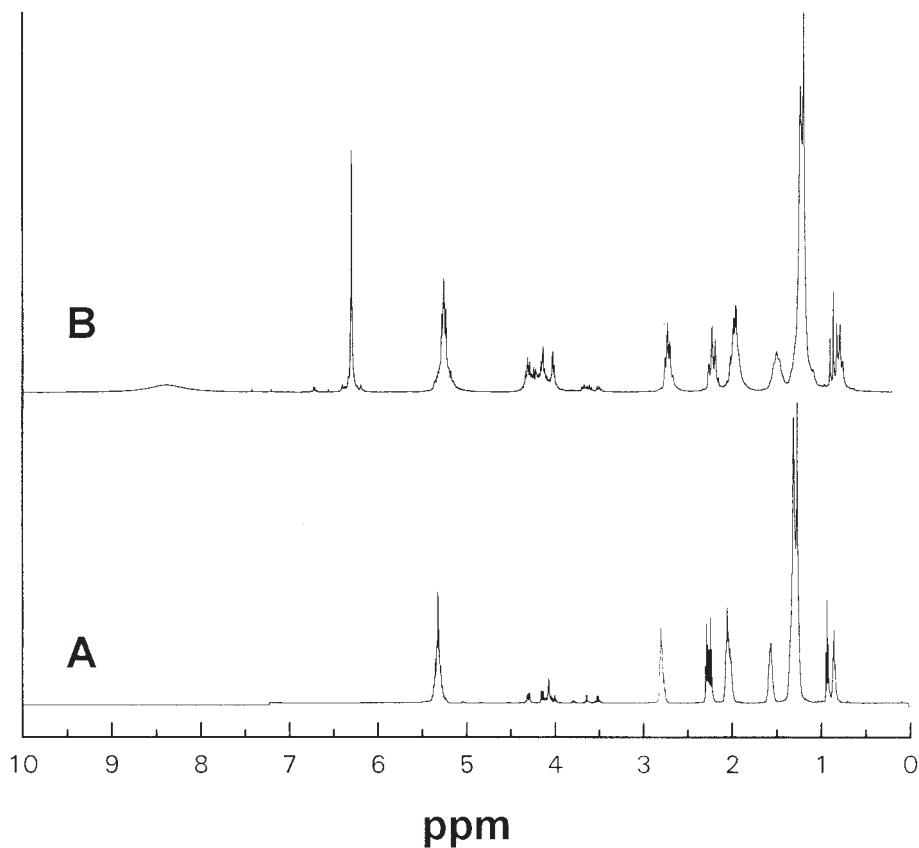

Figure 5 ^{1}H-NMR spectrum of linseed oil (curve A) and LOMG maleate (curve B).

TABLE II
Chemical Shifts for Different Types of Hydrogen Nuclei in Linseed Oil and the Final Resin

Signal (ppm)	Assignment	
	Linseed oil	Final resin
0.9	CH_3—	CH_3—
1.3	—CH_2—	—CH_2—
2	—CH_2—CH=CH—	—CH_2—CH=CH—
2.3	—CH_2—(C=O)—O—	—CH_2—(C=O)—O—
2.8	—CH=CH—CH_2—CH=CH—	—CH=CH—CH_2—CH—CH—
4.2	—CH_2—O—(C=O)	—CH_2—O—(C=O)—
5.1	—CH—O—(C=O)—~	—CH—O—(C=O)—~
5.3	—CH=CH—	—CH=CH—
6.3	—	CH_2—O—(O=C)—CH=CH—(C=O)—OH
8.4	—	CH_2—O—(O=C)—CH=CH—(C=O)—OH

strong decrease of the intensity in the 1779 and 1849 cm^{-1} bands, corresponding to the cyclic maleic anhydride. The peak at 1098 cm^{-1} decreases because of the disappearance of the OH groups in the maleinization reaction to form ester groups.

It was found that the reaction proceeds very fast initially but slows down towards the end. This observation is in agreement with the previous report on soy oil monoglyceride maleates.[7]

Figure 5 shows the ^{1}H-NMR spectrum of linseed oil (curve A) and the LOMG-maleate (curve B) used in the characterization of both materials. The corresponding peak assignments are shown in Table II. The peak corresponding to the oil internal unsaturations is clearly displayed at 5.3 ppm, and it appears with a similar intensity in the spectrum of the final resin. In curve B (resin), a new intense peak at 6.3 ppm is a clear indication of the presence of unsaturation from the maleate moieties. The acid proton signal appears at 8.4 ppm. The increase in the intensity of the peak in the 4–4.5 ppm region, which corresponds to hydrogens associated to ester groups, further confirms the formation of maleate half esters.

At the end of the reaction, an almost negligible fraction of the total maleate unsaturation was found to be isomerized to the fumarate isomer (1.8%), whose chemical shift is around 6.9 ppm.

The calculated signal intensity ratio of maleate protons (6.3 ppm) to fatty acid protons (5.3 ppm) was 0.65. This value is in the range found by other authors.[7] Maximizing this ratio will provide a monomer capable of giving a high density of crosslinking points when polymerized.

Figure 6 shows SEC chromatograms of linseed oil (curve A) and LOMG (curve B). The former shows several peaks corresponding to species eluted at dif-
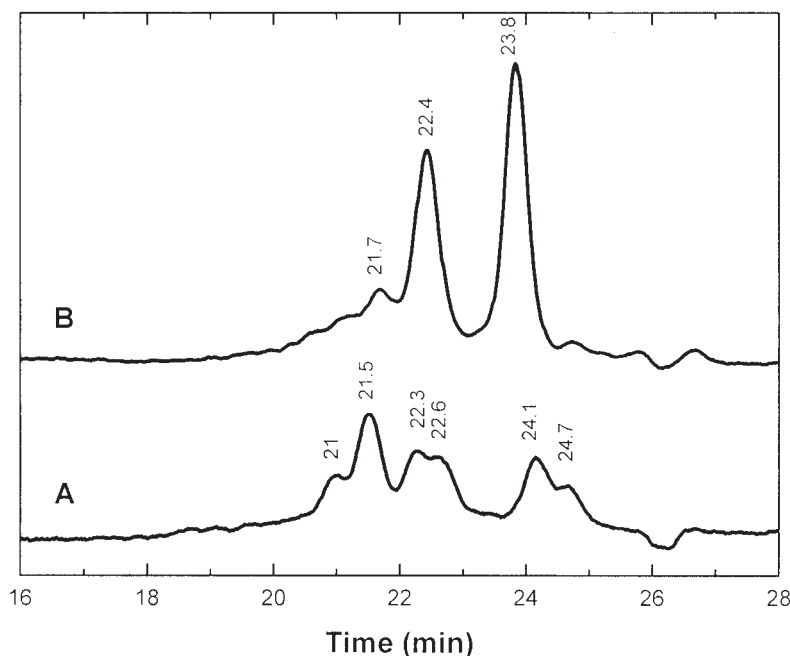

Figure 6 SEC chromatograms of linseed oil (curve A) and LOMG (curve B).
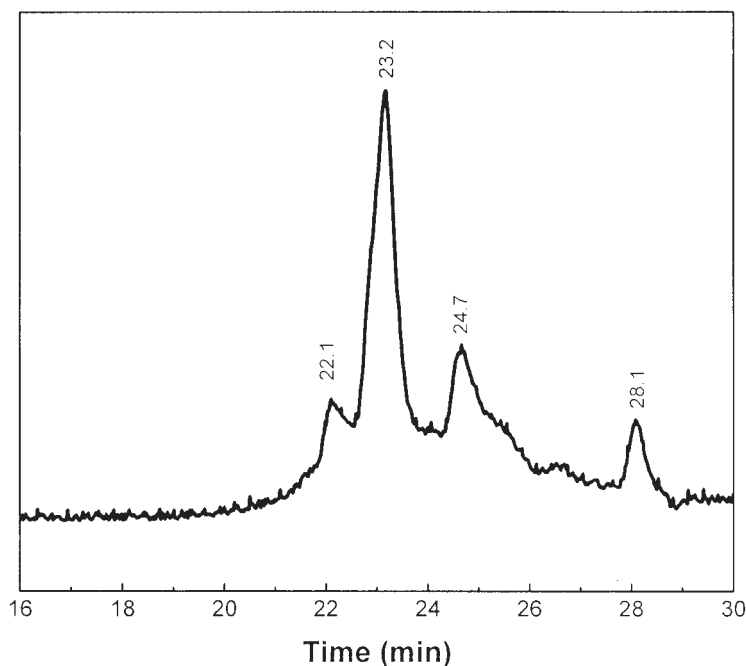
Figure 7 SEC chromatogram of LOMG maleate.

ferent times, 21–21.5, 22.3–22.6, and 24.1–24.7 min, corresponding to triglycerides, diglycerides, and free acids. The product of the glycerolysis reaction is a mixture of a small concentration of triglycerides (peak at 21.7 min), diglycerides (peak at 22.4 min), monoglycerides (peak at 23.8), and glycerol whose signal does not appear in the UV detector.

The advance of the maleinization reaction was followed by size exclusion chromatography (SEC), resulting in a progressive decrease of the peak corresponding to maleic anhydride, which appears at 28 min.

The SEC chromatogram of the final resin confirmed the broad distribution of products (Fig. 7): diglyceride monomaleates and monoglyceride mono and bismaleates (peaks at 22.1 and 23.2), and glycerol tris and bismaleates (peak at 24.7 min). The peak at 28 min shows that maleic anhydride is still present at the end of the reaction.

To quantify the variations in the concentration of ester groups, during the different steps of the resin synthesis, the acid numbers and the saponification values of the samples were determined. Table III shows the results of these measurements. It is clear that the number of ester groups per gram of sample has almost doubled from the initial value of the LOMG as a result of the maleinization.

Dynamic mechanical analysis (DMA)

The resin, synthesized and characterized, was copolymerized with different concentrations of St, and the thermal properties of the resulting materials were analyzed from DMA results.

The storage moduli of the copolymers are shown in Figure 8. It is clear that the copolymers are near the glass-rubber transition zone at room temperature. Moreover, at this temperature, the value of the glassy modulus is a direct function of the concentration of St in the formulation; the higher the St concentration, the higher the modulus. However, at higher temperatures, the rubber modulus is inversely related to the percentage of St (at least up to 60% St). It correlates with the crosslinking density of the material and the rigidity of the crosslinking points, which decrease as more St is introduced to the copolymer and longer St-St sequences are incorporated between the resin crosslinking points.

Figure 9 shows the experimental curves of the damping function, tan δ, of the copolymers at different styrene concentrations. The position of the maximum in the tan δ curve is taken as the glass transition temperature of the samples. The Tg values decrease

TABLE III
Acid Number and Saponification Value and Ester Group Concentrations for Linseed Oil, LOMG, and Final Resin

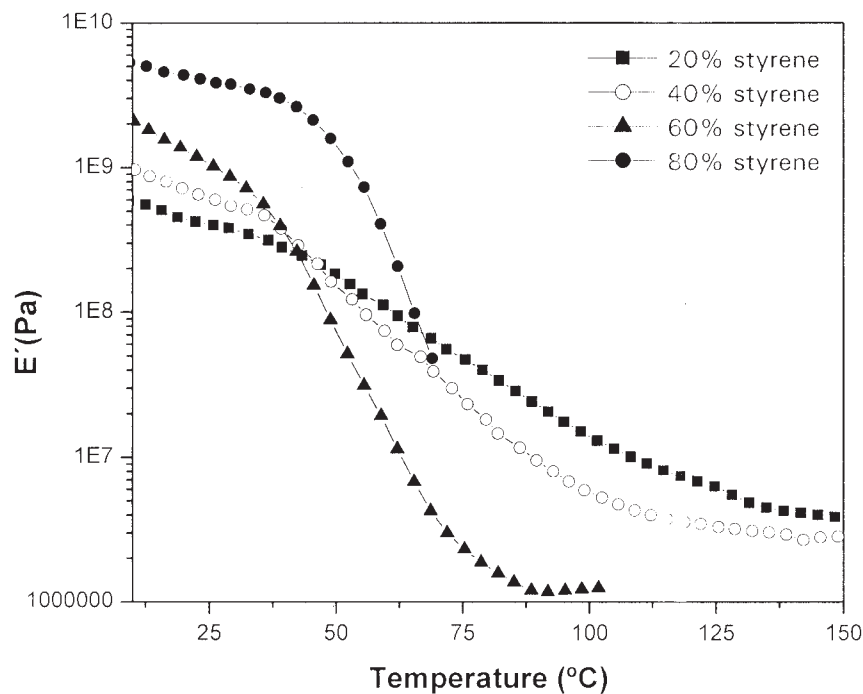|	Acid number (mg KOH/g)	Saponification number (mg KOH/g)	Ester groups (moles/g sample)
Linseed oil	77.44	199.8	0.00218
LOMG	4.07	142.2	0.00246
Final resin	192.83	459.4	0.00475

Figure 8 Storage modulus, E', as a function of the temperature for LOMG maleate/St copolymers of different compositions.

with increasing content of St in the copolymer up to 60%, and then increase. This behavior is the result of counteracting factors: the plasticizing action of the fatty acid chains and the crosslinking structure. The copolymer structure is expected to be similar to synthetic polyester resins, which produce "microgels," with dense material formed by a large proportion of intramolecular reactions, joined by less dense copolymer richer in St. The incorporation of more St usually leads to smaller "microgels" because of the solvent action of the St comonomer. In this last case, the crosslinkages occur through longer St–St sequences and there is a smaller contribution of direct resin-resin linkages or short St sequences links.
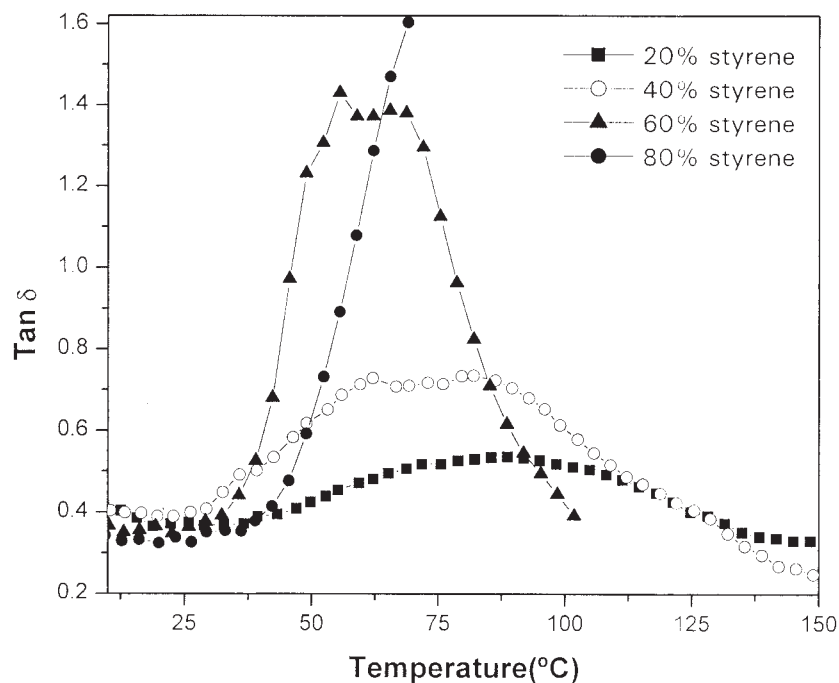

Figure 9 Tan δ as a function of the temperature for LOMG maleate/St copolymers of different compositions.

TABLE IV
Tensile Properties of the Different Copolymers

	Percentage of styrene (by weight)	
	20	40
Tensile modulus (MPa)	140.94 ± 12.27	233.75 ± 7.25
Yield stress (MPa)	5.29 ± 0.20	8.74 ± 0.26
Ultimate stress (MPa)	6.37 ± 0.55	10.59 ± 0.42
Ultimate strain (mm/mm)	0.17 ± 0.05	0.37 ± 0.05
Toughness (MPa)	1.03 ± 0.18	3.30 ± 0.51

Thus, the crosslinking points become more mobile in the network as more St is added. This effect shifts T_g to lower temperatures. On the other hand, at too high St concentrations, the transition becomes more similar to that of the St homopolymer and the T_g shifts back to higher temperatures.

It is also obvious from Figures 8 and 9 that the transition is very broad and begins at low temperatures (close to room temperature). The presence of fatty acids is known to have a plasticizing effect,[2] and this would explain the low temperature relaxations that broaden the glass-rubber transition. Besides, the transition width is broader at low St concentrations. In this content range, high temperature relaxations are also present, which would correspond to less mobile chains and a more heterogeneous network.

Mechanical properties

Linseed oil–styrene copolymers present final properties that can differ from those of the synthetic-based thermoset materials. They are slightly flexible, but break is extremely fragile. However, given their characteristics, they could be tested in tensile, compression, and bending modes.

Tensile properties of the copolymers are shown in Table IV. The samples with 60 and 80% wt. of St were not tested due to their intrinsic fragility. The sample prepared with 40% of St shows higher modulus, higher yield, and ultimate stresses and higher ultimate deformation than the 20% wt. St sample. All these features lead to a material that shows improved tensile toughness, more than three times higher than the 20% sample. However, as mentioned above, higher concentrations of St lead to a rapid deterioration of properties, and tensile testing is not possible.

Figure 10 shows the true stress versus deformation in compression tests, measured for samples made with different weight concentrations of St. The curves for samples made with 20, 40, and 60% of St show stress softening, a general behavior of amorphous glassy polymers, followed by stress hardening. The sample with 80% of St shows behavior similar to that of the polystyrene homopolymer, that is, brittle fracture without any plastic deformation. The modulus increases from 20 to 40% St. Samples prepared with higher concentrations of St do not show a clear trend in this property.

The values of the compressive yield stress, reported in Table V, refer to the intrinsic property of the polymer measured as the maximum of the true stress versus nominal strain ($\Delta\varepsilon/\varepsilon0$), which is related to the start of yielding of the material. The yield stress in-
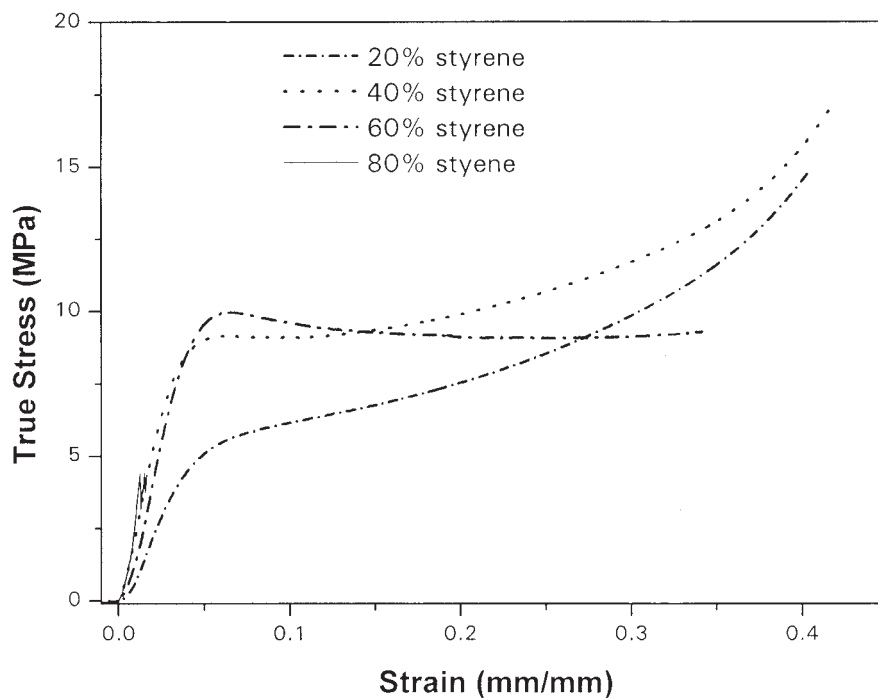

Figure 10 True stress–strain response in compression tests, measured for samples with different weight concentrations of St.

TABLE V
Compressive Properties of the Different Copolymers

	Percentage of styrene (by weight)			
	20	40	60	80
Compressive modulus (MPa)	137.94 ± 21.49	264.45 ± 22.52	251.42 ± 42.47	564.72 ± 9.34
Yield stress (MPa)	5.17 ± 0.64	9.08 ± 0.40	9.25 ± 1.97	—
Ultimate stress (MPa)	12.43 ± 3.24	18.20 ± 3.85	8.96 ± 1.25	4.16 ± 0.26
Ultimate strain (mm/mm)	0.36 ± 0.05	0.42 ± 0.03	0.32 ± 0.06	0.01 ± 0.002

creased with the percentage of St but leveled off at 40–60% St. Finally, due to the fragility of the copolymer prepared with 80% of St, it was impossible to reach yielding in this material. Therefore, it is apparent that a moderate addition of St drastically improves the properties of the end material. On the other hand, breakage shows an optimum at about 40% of St, which is the usual concentration of St found in polyester and vinylester synthetic formulations.

The flexural modulus values of the copolymers, measured in three-point bending tests, are shown in Table VI. There is an overall trend of increasing modulus as St% is increased, which was also the trend observed in DMA measurements. The slight "anomaly" at 40–60% of St, also observed in compression tests, may be the result of the interplay between counteracting effects, crosslinking density, and length of St homopolymer linkages.

Flexural strength data could not be determined because the samples suffered large deformations without breakage.

Fracture behavior

Fractography analysis

Figure 11 shows the optical microscopic analysis of the fracture surfaces of the different samples. This figure reveals differences in the crack propagation mechanisms of the materials obtained with different percentages of St.

None of the samples show any sign of plastic deformation, which is the typical result in brittle fracture and usually found in unmodified crosslinked resins. Visual observation of the fracture surface of the copolymer with 60% of St reveals a very smooth and mirror-like fracture. The copolymers with 20 and 40% of St show arrest of the crack, followed by a region of closely spaced striations parallel to the direction of

crack growth. The 40% of St sample presents a much rougher surface, indicating that more energy was consumed during fracture.

Fracture toughness and Work of Fracture (wof)

The work of fracture gives the energy necessary for driving the crack through the whole sample. The critical energy release rate, or fracture toughness, describes the stage of crack instability.

Differences in fracture propagation mode are not reflected in K_{IC}, and this appears incomplete in describing the whole fracture behavior of these materials. To take into account the differences in the crack propagation mode, the propagation strain energy release rate was also calculated. Montemartini and coworkers[13] reported that the strain energy release rate at its propagation value, the G_{CP} (2wof) approach, resulted in more accurate representation of the actual behavior in a similar material.

In spite of the differences in the two approaches, the fracture tests showed the same tendency in K_{IC} and wof values (Fig. 12). All materials show fragile behavior, in agreement with the visual examination of the fracture surfaces; however, the material prepared with 40% of St displayed maximum toughness. A drastic decrease in the K_{IC} value occurs at 60% of St, in coincidence with the deterioration of mechanical properties. The value corresponding to the sample prepared with 80% of St could not be obtained due to extreme fragility of this material.

It should be noticed that, although the K_{IC} values are very low (particularly for the 20 and 60% of St samples), the values reported are the result of averaging at least eight specimens, obtaining a very low dispersion in the measurements (error bars are included), which allows us to conclude that the observed trend is real in spite of the low values obtained.

TABLE VI
Flexural Properties of the Different Copolymers

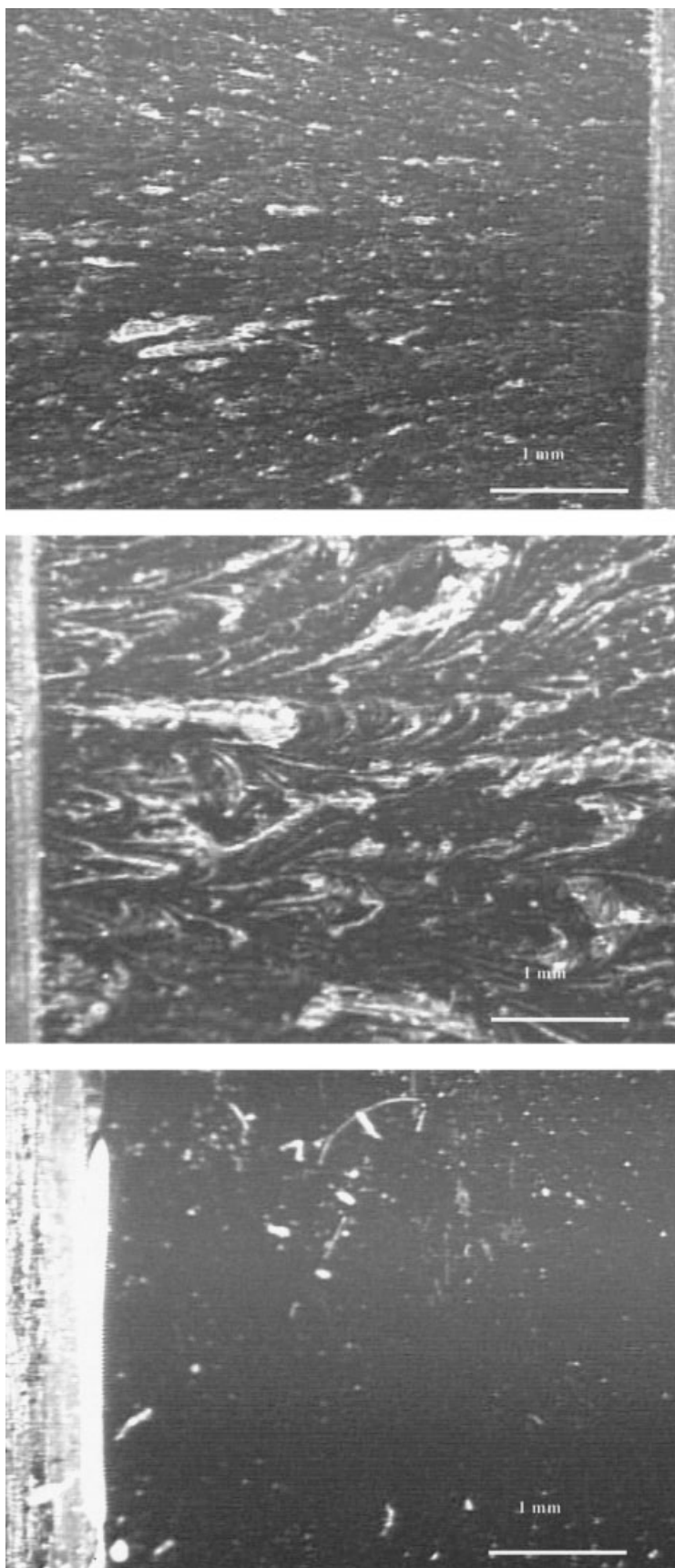|	Percentage of styrene (by weight)			
	20	40	60	80
Flexural modulus (MPa)	171.10 ± 21.19	341.49 ± 45.82	292.84 ± 24.23	507.07 ± 8.93

Figure 11 Fracture surfaces of samples with different percentages by weight of St: (a) 20%, (b) 40%, (c) 60%.
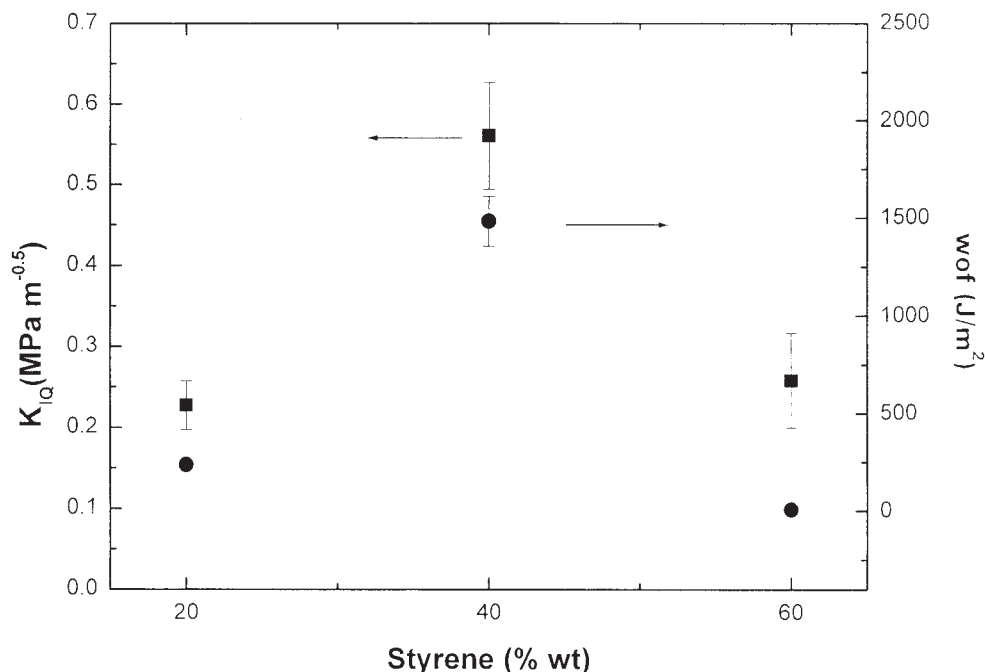
Figure 12 K_{IQ} (■) and WOF (●) values as a function of the percentage of St.

This conclusion is supported by the similar trend obtained by considering the whole energy dissipation during fracture (WOF) and the good agreement with the observation of the corresponding microscopy for the fracture surfaces (Fig. 11) for samples with different percentages of St.

CONCLUSIONS

Polymeric materials from natural resources were obtained and characterized. Glycerolysis and further maleinization of linseed oil was performed and followed by different techniques, such as GPC, FTIR, and H^1NMR. Titration techniques, as well as NMR techniques, indicated that there was an increase in the amount of ester groups after maleinization and showed that the concentration of unreacted maleic anhydride was negligible in the final resin.

The mechanical properties of the maleinized linseed oil–St copolymers were related with their degree of crosslinking and length of St homopolymer sequences. Crosslinking increased the elastic modulus in the rubber region.

The room temperature mechanical properties showed an overall trend of increasing rigidity as the percentage of St is increased, with increasing yield stress in tensile and compression tests up to 40% St.

Fracture tests showed that the copolymer with 40% of St had better fracture behavior with a higher K_{IC}

and WOF value, in agreement with fractography observations and toughness values revealed by the materials in tensile tests.

References

1. Rowell, R. M. Paper and Composites from Agro-Based Resources; Young, R. A.; Rowell, J. K., Eds.; CRC Press: Boca Raton, 1997; Chapter 7, p 249.
2. Khot, S. N.; Lascala, J. J.; Can, E.; Morye, S. S.; Williams, G. I.; Plamese, G. R.; Kusefoglu, S. H.; Wool, R. P. J Appl Polym Sci 2001, 82, 703.
3. Formo, M. W.; Jungermann, E.; Norris, F. A.; Sonntag, N. O. V. Bailey's Industrial Oil and Fat Products; Swern, D., Ed. Wiley: New York, 1985; Vol. 1, 4th ed., Chapter 10, p 749.
4. Li, F.; Larock, R. C. J Appl Polym Sci 2000, 78, 1044.
5. Li, F.; Hanson, M. V.; Larock, R. C. Polymer 2001, 42, 1567.
6. Li, F.; Hasjim, J.; Larock, R. C. J Appl Polym Sci 2003, 90, 1830.
7. Can, E.; Kusefoglu, S.; Wool, R. P. J Appl Polym Sci 2001, 81, 69.
8. Hammond, E. G. Introduction to Fats and Oils Technology; Wan, P. J., Ed.; American Oil Chemists' Society: New Orleans, 1991; Chapter 1, p 8.
9. Urbanski, J. In Handbook of Analysis of Synthetic Polymers and Plastics; Urbanski, J.; Czerwinski, W.; Janicka, K.; Majewska, F.; Zowall, H., Eds.; Wiley: Chichester, 1977; Chapter 1, pp 48–49.
10. Dowling, N. E. Mechanical Behavior of Materials: Engineering Methods for Deformation, Fracture, and Fatigue; Prentice-Hall: Englewood Cliffs, NJ, 1993; Chapter 5, pp 154–155.
11. Shen, J.; Chen, C. C.; Saver, J. A. Polymer 1985, 26, 511.
12. Adams, M. J.; Williams, D.; Williams, J. G. J Mater Sci 1989, 24, 1772.
13. Montemartini, P.; Cuadrado, T.; Frontini, P. J Mater Sci 1999, 10, 309.